INTERNATIONAL JOURNAL FOR NUMERICAL METHODS IN ENGINEERING
Int. J. Numer. Meth. Engng 2014; **97**:111–129
Published online 31 October 2013 in Wiley Online Library (wileyonlinelibrary.com). DOI: 10.1002/nme.4586

Director-based beam finite elements relying on the geometrically exact beam theory formulated in skew coordinates

S. R. Eugster[1,*,†], C. Hesch[2], P. Betsch[2] and Ch. Glocker[1]

[1]*Institute for Mechanical Systems, Center of Mechanics, Department of Mechanical and Process Engineering, ETH Zürich, Switzerland*
[2]*Institute of Mechanics, Karlsruhe Institute of Technology (KIT), Germany*

SUMMARY

In the present work, a new director-based finite element formulation for geometrically exact beams is proposed. The new beam finite element exhibits drastically improved numerical performance when compared with the previously developed director-based formulations. This improvement is accomplished by adjusting the underlying variational beam formulation to the specific features of the director interpolation. In particular, the present approach does not rely on the assumption of an orthonormal director frame. The excellent performance of the new approach is illustrated with representative numerical examples. Copyright © 2013 John Wiley & Sons, Ltd.

Received 12 July 2013; Revised 18 September 2013; Accepted 19 September 2013

KEY WORDS: virtual work; structural mechanics; constrained theories; geometrically exact beam; nonlinear beam elements

1. INTRODUCTION

This work deals with nonlinear beam finite elements emanating from the geometrically exact Simo-Reissner beam model (Simo [1], Reissner [2]). The finite element discretization applied in the present work relies on the interpolation of the director field, in contrast to the use of rotational degrees of freedom or quaternions, see, for example, McRobie & Lasenby [3]. This type of finite element interpolation can be considered as a characteristic feature of continuum-based beam elements and has been applied, among others, in Bathe & Bolourchi [4] and Gruttmann *et al*. [5], see also Chapter 9 in Belytschko *et al*. [6]. The director interpolation has originally been employed in the finite element discretization of the Simo-Reissner beam theory in Romero & Armero [7] and Betsch & Steinmann [8, 9]. Because the director interpolation does not rely on rotational degrees of freedom, it retains the fundamental properties of frame indifference (or objectivity) and conservation of angular momentum in the finite element framework, as shown in [8, 10] . Moreover, it facilitates the straightforward design of structure-preserving time integrators as has been shown in Betsch & Steinmann [9, 11], Armero & Romero [12], and Leyendecker *et al*. [13].

In the director interpolation, the orthonormality of the director frame is typically relaxed to the nodal points of the finite element formulation. That is, the orthonormality of the directors is typically enforced in the nodal points, either by using three rotation parameters or by applying the method of Lagrange multipliers. We refer to [8] where the connection between the two alternative approaches is highlighted.

*Correspondence to: S. R. Eugster, Institute for Mechanical Systems, Center of Mechanics, Department of Mechanical and Process Engineering, ETH Zürich, Switzerland.

†E-mail: eugster@imes.mavt.ethz.ch

The lack of orthonormality of the director frame on element level can be viewed as discretization error that diminishes when the number of elements is increased. Consequently, the corresponding finite element formulation is still consistent with the underlying beam theory. However, as has been observed in [8], to achieve a certain level of accuracy, beam finite elements relying on the director interpolation typically require a larger number of elements when compared with the finite element formulations based on the interpolation of three rotation parameters. Further investigations in this direction can be found in Romero [10] and Bauchau & Han [14].

In the present work, we propose a new finite element implementation of the geometrically exact beam theory. The newly developed formulation relies on the director interpolation and accounts for the lack of orthonormality of the discrete director frame in a natural way. This is achieved by the formulation of the underlying variational equations using convected coordinates. Such a formulation, where covariant and contravariant directors are distinguished, inherently allows for skew coordinate systems. In case the directors are mutually orthonormal, the new formulation boils down to the original version of the geometrically exact beam theory. It turns out that the new approach yields a dramatically improved numerical performance when compared with the original director-based implementation developed in [8].

The quality of the new finite element formulation lies also in the notion that the beam is considered as a constrained three-dimensional continuum. Using the principle of virtual work and the symmetry condition of the stress vector, the variational beam equations are developed merely by kinematical assumptions. This approach guarantees complete consistency between all introduced kinematic and kinetic quantities. Additionally, with a variational formulation of the symmetry condition, the authors never leave the route of a variational formulation of the mechanical problem.

An outline of the rest of the paper is as follows. In Section 2, the fundamental principles of the underlying continuum theory are outlined in a concise manner. The geometrically exact beam theory in skew coordinates is derived in Section 3. In Section 4, we apply a spatial discretization based on finite elements. Representative numerical examples are given in Section 5. Eventually, conclusions are drawn in Section 6.

2. FUNDAMENTAL PRINCIPLES OF A CONTINUOUS BODY

In this section, we summarize the variational form of the continuum mechanical theory that serves as a starting point for the derivation of the beam formulation in the subsequent section. In addition to that we present a derivation of the symmetry condition of the stress vector from the variational form of the law of interaction which is in this form completely new as far as it is known to the authors.

We consider a three-dimensional body $\overline{\mathcal{B}}$ as a three-dimensional smooth manifold with boundary that can be covered by a single chart ϕ, see Figure 1. Hence, every material point $p \in \overline{\mathcal{B}}$ can be described by three coordinates $\left(\theta^1, \theta^2, \theta^3\right) \in \overline{\mathrm{B}} \subset \mathbb{R}^3$ where $\overline{\mathrm{B}} = \phi\left(\overline{\mathcal{B}}\right)$. A configuration $\kappa : \overline{\mathcal{B}} \to \mathbb{E}^3$ is an embedding of the body manifold into the Euclidean three-space $\mathbb{E}^3$. Because the configuration maps the material points p to the Euclidean three-space, which is a vector space, the

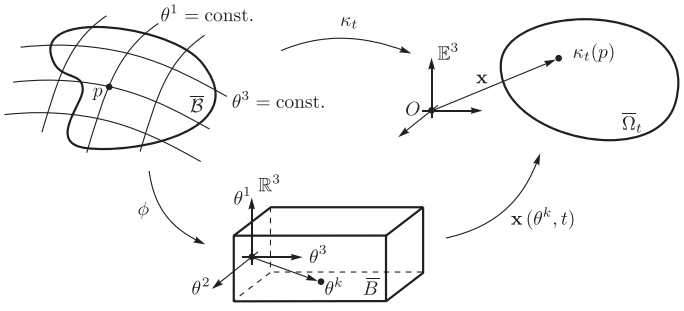

Figure 1. Schematic overview of the kinematics of the body manifold $\overline{\mathcal{B}}$.

DOI: 10.1002/nme

placement of a material point $\kappa(p)$ can be represented by the position vector $\mathbf{x} \in \mathbb{E}^3$. A motion $\kappa_t : \overline{\mathcal{B}} \times \mathbb{R} \to \mathbb{E}^3$ of the body is a differentiable parametrization of configurations with respect to time $t \in \mathbb{R}$. Thus, at a given instant of time t, the subset $\overline{\Omega}_t = \kappa_t\left(\overline{\mathcal{B}}\right) \subset \mathbb{E}^3$ is covered by the body manifold. Using the chart ϕ, the coordinate representation of the motion is the vector valued function

$$\mathbf{x} : \overline{\mathrm{B}} \times \mathbb{R} \to \mathbb{E}^3,\ (\theta^k, t) \mapsto \mathbf{x} = \kappa_t \circ \phi^{-1}(\theta^k) = \mathbf{x}(\theta^k, t)\,, \tag{1}$$

also denoted as the position field. Note that we are using the same symbol for the variables $\mathbf{x}$ as for the functions whose results they are. In the following sections, we will work mainly with the coordinate representation of the motion $\mathbf{x}\left(\theta^k, t\right)$ and will treat motion and coordinate representation of the motion synonymously. A variational family of the motion of the body is a differentiable parametrization of motions $\hat{\mathbf{x}}\left(\theta^k, t, \varepsilon\right)$ with respect to a parameter $\varepsilon \in \mathbb{R}$. The actual time behavior is obtained for $\varepsilon = \varepsilon_0$, that is, $\mathbf{x}\left(\theta^k, t\right) = \hat{\mathbf{x}}\left(\theta^k, t, \varepsilon_0\right)$. Insofar the variation of the position field $\mathbf{x}$ is given as

$$\delta\mathbf{x}(\theta^k, t) = \left.\frac{\partial \hat{\mathbf{x}}}{\partial \varepsilon}\right|_{\varepsilon=\varepsilon_0} \delta\varepsilon\,. \tag{2}$$

Furthermore, we introduce the covariant base vectors $\mathbf{g}_i$, its variation $\delta\mathbf{g}_i$, and its associated contravariant base vectors $\mathbf{g}^i$ for $i \in \{1, 2, 3\}$ according to

$$\mathbf{g}_i = \mathbf{x}_{,i}\ ,\quad \delta\mathbf{g}_i = \delta\mathbf{x}_{,i}\ ,\quad \mathbf{g}^i = g^{-1/2}(\mathbf{g}_j \times \mathbf{g}_k)\,,\quad g^{1/2} = \mathbf{g}_1 \cdot (\mathbf{g}_2 \times \mathbf{g}_3)\,, \tag{3}$$

where partial derivatives $\partial(\bullet)/\partial\theta^k$ are abbreviated by $(\bullet)_{,k}$. The construction of the contravariant basis is valid for even permutations of $\{i, j, k\} = \{1, 2, 3\}$. The contravariant base vectors fulfill the reciprocity condition $\mathbf{g}^i \cdot \mathbf{g}_j = \delta^i_j$. In the following, all vector triads will tacitly be equipped with a contravariant triad as defined in (3). In the remainder of this article, we call quantities with lower index $(\bullet)_i$ covariant and quantities with upper index $(\bullet)^i$ contravariant.

The virtual work principle states that the body $\overline{\mathcal{B}}$ is in the dynamical equilibrium if and only if the virtual work δW vanishes for all virtual displacements $\delta\mathbf{x}$ at any instant of time t, that is,

$$\delta W(\mathbf{x}, \delta\mathbf{x}) = \delta W^{\mathrm{int}} + \delta W^{\mathrm{dyn}} - \delta W^{\mathrm{ext}} - \delta W^{\mathrm{z}} = 0 \quad \forall\delta\mathbf{x}, \forall t\,. \tag{4}$$

Here, δW^{int} represents the contribution of the internal virtual work, which is formulated in the body chart ϕ as

$$\delta W^{\mathrm{int}} = \int_{\overline{\mathrm{B}}} \boldsymbol{\sigma} : (\delta\mathbf{g}_i \otimes \mathbf{g}^i) g^{1/2} \mathrm{d}^3\theta = \int_{\overline{\mathrm{B}}} \mathbf{t}^i \cdot \delta\mathbf{g}_i\, \mathrm{d}^3\theta\,, \tag{5}$$

where $\mathrm{d}^3\theta = \mathrm{d}\theta^1\mathrm{d}\theta^2\mathrm{d}\theta^3$ and summation convention for repeated indices is applied. The stress vector $\mathbf{t}^i\left(\theta^k, t\right)$ can be recognized in the Cauchy stress tensor $\boldsymbol{\sigma}\left(\mathbf{x}\left(\theta^k\right), t\right) = g^{-1/2}\,\mathbf{t}^i \otimes \mathbf{g}_i$. Hence, the stress vector $\mathbf{t}^i$ is the traction in the current configuration that acts at the surface element $\mathbf{g}_j \times \mathbf{g}_k \mathrm{d}\theta^j \mathrm{d}\theta^k = \mathbf{g}^i g^{1/2} \mathrm{d}\theta^j \mathrm{d}\theta^k$ for even permutations of the indices $\{i, j, k\} = \{1, 2, 3\}$. An analogous formulation of the internal virtual work (5) can be found, for example, in Chapter 16 of Antman [15].

The contributions of the inertia terms, the external forces $\mathrm{d}\mathbf{f}$, and the perfect bilateral constraint forces $\mathrm{d}\mathbf{z}$ are

$$\delta W^{\mathrm{dyn}} = \int_{\overline{\mathrm{B}}} \delta\mathbf{x} \cdot \ddot{\mathbf{x}}\, \mathrm{d}m\,,\quad \delta W^{\mathrm{ext}} = \int_{\overline{\mathrm{B}}} \delta\mathbf{x} \cdot \mathrm{d}\mathbf{f}\,,\quad \delta W^{\mathrm{z}} = \int_{\overline{\mathrm{B}}} \delta\mathbf{x} \cdot \mathrm{d}\mathbf{z}\,, \tag{6}$$

where $\dot{(\bullet)}$ denotes the total time derivative. We consider the mass distribution $\mathrm{d}m$ and the force distributions $\mathrm{d}\mathbf{f}$ and $\mathrm{d}\mathbf{z}$ as measures allowing for Dirac-type contributions as well. The perfect bilateral constraint forces $\mathrm{d}\mathbf{z}$ are defined by the principle of d'Alembert-Lagrange, stating that the virtual

DOI: 10.1002/nme

work of the perfect bilateral constraint forces integrated over the total mechanical system, that is the body $\overline{\mathcal{B}}$, vanishes for all admissible virtual displacements $\delta\mathbf{x}_{\text{adm}}$. Virtual displacements are called admissible if they do not violate the perfect bilateral constraints. Hence, the principle of virtual work can be expressed in the body chart as follows.

Theorem 1 (Principle of Virtual Work)
A body $\overline{\mathcal{B}}$ is in the dynamical equilibrium if and only if the virtual work expression vanishes for all admissible virtual displacements $\delta\mathbf{x}_{\text{adm}}$ at any instant of time t, that is,

$$\delta W = \int_{\overline{\mathrm{B}}} \mathbf{t}^i \cdot \delta\mathbf{g}_i \,\mathrm{d}^3\theta + \int_{\overline{\mathrm{B}}} \delta\mathbf{x} \cdot \ddot{\mathbf{x}} \,\mathrm{d}m - \int_{\overline{\mathrm{B}}} \delta\mathbf{x} \cdot \mathrm{d}\mathbf{f} = 0 \quad \forall \delta\mathbf{x} = \delta\mathbf{x}_{\text{adm}}, \forall t \,. \tag{7}$$

Besides the virtual work principle, the law of interaction for internal forces has to be respected (cf. Section 2 of Glocker [16]), which coincides in its variational form with the 'Axiom of Power of Internal Forces' formulated by Germain [17]. The variational form of the law of interaction states that the internal virtual work (5) of any subbody $\mathcal{B}' \subset \overline{\mathcal{B}}$ is unaffected and therefore invariant with respect to all Euclidean transformations. The transformed position field takes the form $\mathbf{x}^+ = \mathbf{Q}\mathbf{x} + \mathbf{c}$ where $\mathbf{Q} \in SO(3)$ is a special orthogonal tensor satisfying $\mathbf{Q}^{\mathrm{T}}\mathbf{Q} = \mathbf{Q}\mathbf{Q}^{\mathrm{T}} = \mathbf{I}$, where $\mathbf{I}$ is the second order identity tensor, and $\mathbf{c}$ is a vector of the Euclidean vector space $\mathbb{E}^3$. The rotation $\mathbf{Q}$ and the translation $\mathbf{c}$ are homogenous for the whole subbody $\mathcal{B}'$. Hence, the virtual displacement of the transformed position field is $\delta\mathbf{x}^+ = \delta\mathbf{Q}\mathbf{x} + \mathbf{Q}\delta\mathbf{x} + \delta\mathbf{c}$. The transformed stress vector $\left(\mathbf{t}^i\right)^+$ and the partial derivative of the virtual displacement are given by

$$\left(\mathbf{t}^i\right)^+ = \mathbf{Q}\mathbf{t}^i \,, \quad \delta\mathbf{g}_i^+ = \left(\delta\mathbf{x}^+\right)_{,i} = \delta\mathbf{Q}\mathbf{g}_i + \mathbf{Q}\delta\mathbf{g}_i \,. \tag{8}$$

Hence, we write the law of interaction for an arbitrary subbody $\mathcal{B}' \subset \overline{\mathcal{B}}$ in the body chart ϕ as

$$\begin{aligned} \int_{\mathrm{B}'} \mathbf{t}^i \cdot \delta\mathbf{g}_i \,\mathrm{d}^3\theta &= \int_{\mathrm{B}'} \left(\mathbf{t}^i\right)^+ \cdot \delta\mathbf{g}_i^+ \,\mathrm{d}^3\theta = \int_{\mathrm{B}'} \left(\mathbf{Q}\mathbf{t}^i\right) \cdot (\delta\mathbf{Q}\mathbf{g}_i + \mathbf{Q}\delta\mathbf{g}_i)\mathrm{d}^3\theta \\ &= \int_{\mathrm{B}'} \mathbf{t}^i \cdot \mathbf{Q}^{\mathrm{T}}\delta\mathbf{Q}\,\mathbf{g}_i \mathrm{d}^3\theta + \int_{\mathrm{B}'} \mathbf{t}^i \cdot \delta\mathbf{g}_i \,\mathrm{d}^3\theta \\ &= \delta\mathbf{w} \cdot \int_{\mathrm{B}'} \mathbf{g}_i \times \mathbf{t}^i \,\mathrm{d}^3\theta + \int_{\mathrm{B}'} \mathbf{t}^i \cdot \delta\mathbf{g}_i \,\mathrm{d}^3\theta \,, \end{aligned} \tag{9}$$

where $B' = \phi(\mathcal{B}')$. Because $\mathbf{Q}^{\mathrm{T}}\delta\mathbf{Q}$ is a skew-symmetric tensor, we introduce in the last line of (9) the associated axial vector $\delta\mathbf{w} \in \mathbb{E}^3$, defined by the cross product as $\delta\mathbf{w} \times \mathbf{a} = \mathbf{Q}^{\mathrm{T}}\delta\mathbf{Q}\mathbf{a}$ for all $\mathbf{a} \in \mathbb{E}^3$. The law of interaction requires now the first term on the last line of (9) to vanish for all $\delta\mathbf{Q}$ and consequently for all $\delta\mathbf{w}$. Because the considered mechanical system is a continuous body and the law of interaction has to be fulfilled for any subsystem $\mathcal{B}' \subset \overline{\mathcal{B}}$, the law of interaction in the body chart ϕ coincides with the symmetry condition of the Cauchy stress tensor.

Theorem 2 (Law of Interaction)
As an internal force the stress vector $\mathbf{t}^i$ has to fulfill the symmetry condition in every material point θ^k, that is,

$$\mathbf{g}_i \times \mathbf{t}^i = \mathbf{0} \quad \forall \theta^k \in \overline{\mathrm{B}} \,. \tag{10}$$

3. GEOMETRICALLY EXACT BEAM

In this section, we treat the theory of the geometrically exact beam, also known as the special Cosserat beam, introduced by [2] and [1]. The theory is developed by restricting the kinematics of the three-dimensional continuum to a beam-like kinematic. By inserting the reduced kinematics

DOI: 10.1002/nme

into the virtual work of the continuum, we deduce the virtual work of the beam. From the virtual work of the beam, we then obtain directly the equations of motion of the beam and the corresponding boundary conditions. Throughout our developments, we pay attention to distinguish properly between covariant and contravariant base vectors. As will be shown through the numerical examples presented in Section 5, the newly proposed approach yields a significant improvement over previously developed finite element formulations that do not rely on the distinction between covariant and contravariant base vectors.

3.1. Kinematical assumptions

We define the geometrically exact beam $\overline{\mathcal{B}}$ as a structural element that has a special configuration, that is a reference configuration, where the beam is a three-dimensional body with the position field

$$\mathbf{X}(\theta^\alpha, s) = \boldsymbol{\varphi}_0(s) + \theta^\alpha \mathbf{D}_\alpha(s) \,. \tag{11}$$

In this configuration, as depicted in Figure 2, an appropriate chart ϕ gives us the body coordinates $\theta^i = (\theta^\alpha, s) \in \overline{\mathrm{B}}\,(i = 1, 2, 3\,;\, \alpha = 1, 2)$, which are referred to as convected coordinates. The space curve $\boldsymbol{\varphi}_0(s) = \mathbf{X}(0, 0, s)$ is the reference curve of the beam and is bounded by its ends $s = s_1$ and $s = s_2$ for $s_2 > s_1$. At every material point s of the reference curve $\boldsymbol{\varphi}_0$, we have attached a positively oriented orthonormal director triad $\{\mathbf{D}_k\}$. The two directors $\mathbf{D}_\alpha$ span the plane cross section of the beam. The area of the cross section is parametrized by the coordinates $(\theta^1, \theta^2) \in \bar{A}(s)$. The director triad $\{\mathbf{D}_k\}$ can be related to an orthonormal basis $\{\mathbf{e}_k\}$ fixed in space by introducing the rotation tensor $\mathbf{R}_0(s) \in SO(3)$ such that

$$\mathbf{D}_k(s) = \mathbf{R}_0(s)\mathbf{e}_k \,, \quad \text{with } \mathbf{R}_0 = \mathbf{D}_k \otimes \mathbf{e}^k \,. \tag{12}$$

According to Section 2, the beam is in its reference configuration, a three-dimensional body. This implies bijectivity of the position field $\mathbf{X}(\theta^\alpha, s)$. Because of the kinematical constraints (11), it can happen that interpenetration occurs when the beam is curved too much or the cross sections are too large, compare with Chapter 5 of Rubin [18]. As in the three-dimensional theory, we exclude for the reference configuration interpenetration that is expressed mathematically as $\mathbf{X}_{,1} \cdot (\mathbf{X}_{,2} \times \mathbf{X}_{,3}) > 0$ for all $\theta^i \in \overline{\mathrm{B}}$. That is the reason why beam theories are generally related to slender bodies.

The motion of the geometrically exact beam is the restricted position field

$$\mathbf{x}(\theta^\alpha, s, t) = \boldsymbol{\varphi}(s, t) + \theta^\alpha \mathbf{d}_\alpha(s, t) \,. \tag{13}$$

We call the space curve $\boldsymbol{\varphi}(s, t) = \mathbf{x}(0, 0, s, t)$, which is a bijective function of s and time t, the center line of the beam. At each material point of the center line $\boldsymbol{\varphi}$, we have attached a positively oriented orthonormal director triad $\{\mathbf{d}_k\}$, which is related to the basis $\{\mathbf{e}_k\}$ by introducing the rotation tensor $\mathbf{R}(s, t) \in SO(3)$ such that

$$\mathbf{d}_k(s) = \mathbf{R}(s, t)\mathbf{e}_k \,, \quad \text{with } \mathbf{R} = \mathbf{d}_k \otimes \mathbf{e}^k \,. \tag{14}$$

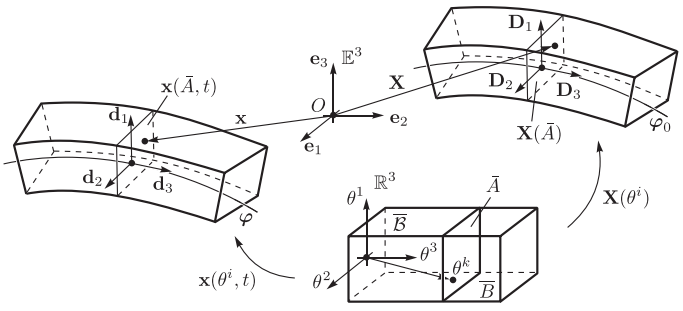

Figure 2. Reference and current configuration of the beam.

DOI: 10.1002/nme

The directors $\mathbf{d}_\alpha$ describe the current state of the cross section $\mathbf{x}(\bar{A}(s),t)$. In the current configuration, we merely ask the center line $\boldsymbol{\varphi}$ to be a bijective function. That means, interpenetration of the cross sections may occur. Insofar, the beam is strictly speaking not a three-dimensional body anymore but a one-dimensional body. Because every material point can be addressed by the convected coordinates θ^k and the variations $\delta\mathbf{x}$ have to comply with the restricted kinematics (13), the dynamics of the constrained system can be derived by the principle of virtual work (7).

In the following, we introduce the effective curvature, the angular velocity, and the virtual rotation. All three objects describe the change of the directors when changing a single parameter as, for example, the parameter s. Using (14), the effective curvature $\tilde{\mathbf{k}}$ is obtained by

$$(\mathbf{d}_k)_{,s} = (\mathbf{R}(s,t)\mathbf{e}_k)_{,s} = \mathbf{R}_{,s}\,\mathbf{R}^{-1}\mathbf{d}_k = \tilde{\mathbf{k}}\mathbf{d}_k\,, \quad \text{with } \tilde{\mathbf{k}} = \mathbf{R}_{,s}\,\mathbf{R}^{-1}\,. \tag{15}$$

Because the present finite element formulation (see Section 4) relies on the nodal interpolation of the director frame, the directors generally do not span an orthornormal basis anymore. That is, on element level the metric coefficients $d^{ij} = \mathbf{d}^i \cdot \mathbf{d}^j$ and $d_{ij} = \mathbf{d}_i \cdot \mathbf{d}_j$ in general do not coincide with the Kronecker delta δ_{ij}. In other words, on element level, the tensor $\mathbf{R}$ introduced in (14) generally does not belong to the special orthogonal group. Inspired by this observation, we relax the orthonormality condition on the director frame and consider metric coefficients that are merely assumed to be constant. Under this condition, the tensor $\tilde{\mathbf{k}}$ still remains skew-symmetric. This is shown in the Appendix. Hence, the skew-symmetric effective curvature $\tilde{\mathbf{k}}$ has an associated axial vector $\mathbf{k} \in \mathbb{E}^3$ so that

$$(\mathbf{d}_k)_{,s} = \tilde{\mathbf{k}}\mathbf{d}_k = \mathbf{k} \times \mathbf{d}_k\,, \quad \text{with } \tilde{\mathbf{k}} = \mathbf{R}_{,s}\,\mathbf{R}^{-1} = \mathbf{d}_{i,s} \otimes \mathbf{d}^i\,. \tag{16}$$

Later in this paper, we are interested in the contravariant components of the effective curvature, which can be written as (cf. Schade & Neemann [19])

$$k^i = \frac{1}{2}e^{ijk}(\tilde{\mathbf{k}})_{kj} = \frac{1}{2}e^{ijk}(\mathbf{d}_k \cdot \mathbf{d}_{j,s})\,, \quad \text{with } e^{ijk} = d^{-1/2}\varepsilon_{ijk}, \tag{17}$$

where ε_{ijk} are the alternating symbols and

$$d^{1/2} = \mathbf{d}_1 \cdot (\mathbf{d}_2 \times \mathbf{d}_3)\,. \tag{18}$$

Analogously to (16), we introduce the angular velocity $\tilde{\boldsymbol{\omega}}$ and its associated axial vector $\boldsymbol{\omega}$ as

$$(\mathbf{d}_k)_{,t} = \tilde{\boldsymbol{\omega}}\mathbf{d}_k = \boldsymbol{\omega} \times \mathbf{d}_k\,, \quad \text{with } \tilde{\boldsymbol{\omega}} = \mathbf{R}_{,t}\,\mathbf{R}^{-1} = \mathbf{d}_{i,t} \otimes \mathbf{d}^i\,. \tag{19}$$

In the same manner, as for the effective curvature and the angular velocity, we obtain the virtual rotation $\delta\tilde{\boldsymbol{\phi}}$ when changing the variational parameter ε.

$$\delta\mathbf{d}_k = \delta\tilde{\boldsymbol{\phi}}\mathbf{d}_k = \delta\boldsymbol{\phi} \times \mathbf{d}_k\,, \quad \text{with } \delta\tilde{\boldsymbol{\phi}} = \delta\mathbf{R}\mathbf{R}^{-1} = \delta\mathbf{d}_i \otimes \mathbf{d}^i\,,\ \delta\boldsymbol{\phi} = \frac{1}{2}\mathbf{d}^i \times \delta\mathbf{d}_i\,. \tag{20}$$

The last expression of the virtual rotation vector is motivated by the following identity and is used in the sequel for the director formulation.

$$\mathbf{d}^i \times \delta\mathbf{d}_i = \mathbf{d}^i \times (\delta\boldsymbol{\phi} \times \mathbf{d}_i) \overset{(A.3)}{=} (\mathbf{d}^i \cdot \mathbf{d}_i)\delta\boldsymbol{\phi} - (\mathbf{d}^i \cdot \delta\boldsymbol{\phi})\mathbf{d}_i = 3\delta\boldsymbol{\phi} - \delta\boldsymbol{\phi} = 2\delta\boldsymbol{\phi}\,. \tag{21}$$

The velocity and acceleration fields are introduced by taking the total time derivative of the position field (13) and the kinematical relation introduced in (19).

$$\dot{\mathbf{x}} = \dot{\boldsymbol{\varphi}} + \boldsymbol{\omega} \times (\mathbf{x} - \boldsymbol{\varphi}) = \dot{\boldsymbol{\varphi}} + \boldsymbol{\omega} \times \boldsymbol{\rho}\,, \quad \text{with } \boldsymbol{\rho} = \mathbf{x} - \boldsymbol{\varphi} = \theta^\alpha\mathbf{d}_\alpha\,, \tag{22}$$

$$\ddot{\mathbf{x}} = \ddot{\boldsymbol{\varphi}} + \dot{\boldsymbol{\omega}} \times \boldsymbol{\rho} + \boldsymbol{\omega} \times (\boldsymbol{\omega} \times \boldsymbol{\rho})\,. \tag{23}$$

With regard to (13) and (16), the partial derivatives of the position field assume the form

$$\mathbf{g}_\alpha = \mathbf{x}_{,\alpha} = \mathbf{d}_\alpha\,, \quad \mathbf{g}_3 = \mathbf{x}_{,s} = \boldsymbol{\varphi}_{,s} + \mathbf{k} \times \boldsymbol{\rho}\,. \tag{24}$$

DOI: 10.1002/nme

Using (13), (20) and (24), the variation of the position field and its partial derivatives are given by

$$\delta\mathbf{x} = \delta\boldsymbol{\varphi} + \delta\boldsymbol{\phi}\times\boldsymbol{\rho}\,, \quad \delta\mathbf{g}_\alpha = \delta\boldsymbol{\phi}\times\mathbf{g}_\alpha\,, \quad \delta\mathbf{g}_3 = \delta\boldsymbol{\varphi}_{,s} + \delta\mathbf{k}\times\boldsymbol{\rho} + \mathbf{k}\times(\delta\boldsymbol{\phi}\times\boldsymbol{\rho})\,. \tag{25}$$

In the Appendix, we verify the important identity

$$(\delta\boldsymbol{\phi})_{,s} = \delta\mathbf{k} - \delta\boldsymbol{\phi}\times\mathbf{k}\,, \tag{26}$$

which is obtained by the fact that the derivative with respect to s and the variation commute, that is, $(\delta\mathbf{d}_k)_{,s} = \delta(\mathbf{d}_k)_{,s}$.

3.2. Virtual work and equations of motion

With the kinematical assumption (13), we impose in fact infinitely many perfect bilateral constraints $\Phi(\theta^\alpha, s, t) = \mathbf{x} - \boldsymbol{\varphi} - \theta^\alpha\mathbf{d}_\alpha = \mathbf{0}$ on the system. The admissible virtual displacements $\delta\mathbf{x}_{\text{adm}}$ are all variations of the reduced kinematics $\mathbf{x}$, that is, $\delta\mathbf{x}_{\text{adm}} = \delta\mathbf{x}$. Because the variations of $\mathbf{x}$ are admissible with respect to the constraints $\Phi = \mathbf{0}$, all corresponding constraint forces are projected out and will not appear in the equations of motion. In the following, we reformulate the virtual work expression (7) by taking into account the reduced kinematics of the beam. In this way, we identify the kinematic quantities of the beam and the corresponding kinetic quantities, that is, the resultant contact force $\mathbf{n}$ and the resultant contact torque $\mathbf{m}$. Furthermore, by assuming a hyperelastic material behavior, appropriate strain measures are identified.

Using (5), (25), and the property of the cross product of (A.2), the internal virtual work density can be written as

$$\mathbf{t}^i\cdot\delta\mathbf{g}_i = \delta\boldsymbol{\phi}\cdot(\mathbf{g}_\alpha\times\mathbf{t}^\alpha) + \mathbf{t}^3\cdot\delta\boldsymbol{\varphi}_{,s} + \delta\mathbf{k}\cdot\left(\boldsymbol{\rho}\times\mathbf{t}^3\right) + \mathbf{t}^3\cdot[\mathbf{k}\times(\delta\boldsymbol{\phi}\times\boldsymbol{\rho})]\,. \tag{27}$$

Employing the symmetry condition (10), we can rewrite the first term in (27) as follows.

$$\delta\boldsymbol{\phi}\cdot(\mathbf{g}_\alpha\times\mathbf{t}^\alpha) \overset{(10)}{=} -\delta\boldsymbol{\phi}\cdot\left(\mathbf{g}_3\times\mathbf{t}^3\right) \overset{(24,A.2)}{=} -\mathbf{t}^3\cdot[\delta\boldsymbol{\phi}\times\boldsymbol{\varphi}_{,s} + \delta\boldsymbol{\phi}\times(\mathbf{k}\times\boldsymbol{\rho})]\,. \tag{28}$$

Using the relation (28) and the Jacobi identity (A.1), we can manipulate (27) further to obtain

$$\begin{aligned}
\mathbf{t}^i\cdot\delta\mathbf{g}_i &= -\mathbf{t}^3\cdot[\delta\boldsymbol{\phi}\times\boldsymbol{\varphi}_{,s} + \delta\boldsymbol{\phi}\times(\mathbf{k}\times\boldsymbol{\rho})] + \mathbf{t}^3\cdot\delta\boldsymbol{\varphi}_{,s}\\
&\quad + \delta\mathbf{k}\cdot\left(\boldsymbol{\rho}\times\mathbf{t}^3\right) + \mathbf{t}^3\cdot[\mathbf{k}\times(\delta\boldsymbol{\phi}\times\boldsymbol{\rho})]\\
&= \mathbf{t}^3\cdot[\delta\boldsymbol{\varphi}_{,s} - \delta\boldsymbol{\phi}\times\boldsymbol{\varphi}_{,s}] + \delta\mathbf{k}\cdot\left(\boldsymbol{\rho}\times\mathbf{t}^3\right)\\
&\quad + \mathbf{t}^3\cdot[\mathbf{k}\times(\delta\boldsymbol{\phi}\times\boldsymbol{\rho}) + \delta\boldsymbol{\phi}\times(\boldsymbol{\rho}\times\mathbf{k})]\\
&\overset{(A.1)}{=} \mathbf{t}^3\cdot[\delta\boldsymbol{\varphi}_{,s} - \delta\boldsymbol{\phi}\times\boldsymbol{\varphi}_{,s}] + \delta\mathbf{k}\cdot\left(\boldsymbol{\rho}\times\mathbf{t}^3\right) + \mathbf{t}^3\cdot[\boldsymbol{\rho}\times(\delta\boldsymbol{\phi}\times\mathbf{k})]\\
&\overset{(A.2)}{=} \mathbf{t}^3\cdot[\delta\boldsymbol{\varphi}_{,s} - \delta\boldsymbol{\phi}\times\boldsymbol{\varphi}_{,s}] + \left(\boldsymbol{\rho}\times\mathbf{t}^3\right)\cdot[\delta\mathbf{k} - \delta\boldsymbol{\phi}\times\mathbf{k}]\,.
\end{aligned} \tag{29}$$

Because the kinematical quantities in the squared brackets depend merely on s, we split the integration over $\overline{\mathrm{B}}$ in an integration over the cross section in the body chart $\bar{\mathrm{A}}(s)$ and an integration along $s\in[s_1, s_2]$.

$$\delta W^{\text{int}} = \int_{\overline{\mathrm{B}}}\mathbf{t}^i\cdot\delta\mathbf{g}_i\,\mathrm{d}^3\theta \overset{(29)}{=} \int_{s_1}^{s_2}\{\mathbf{n}\cdot[\delta\boldsymbol{\varphi}_{,s} - \delta\boldsymbol{\phi}\times\boldsymbol{\varphi}_{,s}] + \mathbf{m}\cdot[\delta\mathbf{k} - \delta\boldsymbol{\phi}\times\mathbf{k}]\}\,\mathrm{d}s\,. \tag{30}$$

The integrated kinetic quantities $\mathbf{n}$ and $\mathbf{m}$ are the resultant contact force and the resultant contact torque of the current configuration defined by

$$\mathbf{n}(s,t) = \int_{\bar{\mathrm{A}}}\mathbf{t}^3\,\mathrm{d}^2\theta\,, \quad \mathbf{m}(s,t) = \int_{\bar{\mathrm{A}}}\left(\boldsymbol{\rho}\times\mathbf{t}^3\right)\,\mathrm{d}^2\theta\,, \tag{31}$$

with the surface element $\mathrm{d}^2\theta = \mathrm{d}\theta^1\mathrm{d}\theta^2$. For the sake of clarity, the contributions due to external forces and inertia are developed in compact form in the Appendix.

DOI: 10.1002/nme

Taking all the modified contributions of the virtual work (30), (A.13), and (A.18), the principle of virtual work (7) leads to

$$\begin{aligned}\delta W = \int_{s_1}^{s_2} \Big\{ \mathbf{n} \cdot [\delta \boldsymbol{\varphi}_{,s} - \delta \boldsymbol{\phi} \times \boldsymbol{\varphi}_{,s}] + \mathbf{m} \cdot [\delta \mathbf{k} - \delta \boldsymbol{\phi} \times \mathbf{k}] + \delta \boldsymbol{\varphi} \cdot \left(A_\rho \ddot{\boldsymbol{\varphi}} + \ddot{\mathbf{q}} - \overline{\mathbf{n}} \right) \\ + \delta \boldsymbol{\phi} \cdot \left(\mathbf{q} \times \ddot{\boldsymbol{\varphi}} + \dot{\mathbf{h}} - \overline{\mathbf{m}} \right) \Big\} \, \mathrm{d}s - (\delta \boldsymbol{\varphi} \cdot \overline{\mathbf{n}} + \delta \boldsymbol{\phi} \cdot \overline{\mathbf{m}})|_{s_1}^{s_2} = 0 \quad \forall \delta \boldsymbol{\varphi}, \delta \boldsymbol{\phi}, t \, .\end{aligned} \tag{32}$$

Using the identity (26) and integration by parts, the virtual work can be expressed as

$$\begin{aligned}\delta W = \int_{s_1}^{s_2} \left\{ \delta \boldsymbol{\varphi} \cdot \left(A_\rho \ddot{\boldsymbol{\varphi}} + \ddot{\mathbf{q}} - \overline{\mathbf{n}} - \mathbf{n}_{,s} \right) + \delta \boldsymbol{\phi} \cdot \left(\mathbf{q} \times \ddot{\boldsymbol{\varphi}} + \dot{\mathbf{h}} - \overline{\mathbf{m}} - \mathbf{m}_{,s} - \boldsymbol{\varphi}_{,s} \times \mathbf{n} \right) \right\} \mathrm{d}s \\ + (\delta \boldsymbol{\varphi} \cdot (\mathbf{n} - \overline{\mathbf{n}}) + \delta \boldsymbol{\phi} \cdot (\overline{\mathbf{m}} - \mathbf{m})) \, |_{s_1}^{s_2} = 0 \quad \forall \delta \boldsymbol{\varphi}, \delta \boldsymbol{\phi}, t \, .\end{aligned} \tag{33}$$

This is the variational expression of the BVP in the current configuration of the geometrically exact beam as derived from the balance laws in Chapter 8 of Antman [15], that is,

$$\begin{aligned}\mathbf{n}_{,s} + \overline{\mathbf{n}} &= A_\rho \ddot{\boldsymbol{\varphi}} + \ddot{\mathbf{q}} \, , \\ \mathbf{m}_{,s} + \boldsymbol{\varphi}_{,s} \times \mathbf{n} + \overline{\mathbf{m}} &= \mathbf{q} \times \ddot{\boldsymbol{\varphi}} + \dot{\mathbf{h}} \, .\end{aligned} \tag{34}$$

with the boundary conditions $\mathbf{n} = \overline{\mathbf{n}}$ and $\mathbf{m} = \overline{\mathbf{m}}$ for $s = \{s_1, s_2\}$.

3.3. Constitutive law

We assume the constitutive law to be hyperelastic. Thus, there exists an elastic potential $W(s)$ such that

$$\delta W^{\mathrm{int}} = \delta \int_{s_1}^{s_2} W(s) \mathrm{d}s \, . \tag{35}$$

We formulate the elastic potential as an additive split of two potentials

$$W(s) = W\left(\gamma_i, k^i\right) = W_1(\gamma_i) + W_2\left(k^i\right) \, , \tag{36}$$

each of which depends on the strain measures γ_i and k^i, respectively. The effective reference curvature is defined as $\tilde{\mathbf{k}}_0(s) = \mathbf{R}_{0,s} \, \mathbf{R}_0^{-1} = \mathbf{D}_{i,s} \otimes \mathbf{D}^i$. The covariant strain

$$\gamma_i(s,t) = \mathbf{d}_i \cdot \boldsymbol{\varphi}_{,s} - \mathbf{D}_i \cdot \boldsymbol{\varphi}_{0,s} \, , \tag{37}$$

measures the difference between the deformation of the center line in the direction $\mathbf{d}_i$ and the deformation of the reference curve in direction $\mathbf{D}_i$. When measuring the difference between the effective curvature and the effective reference curvature in the direction $\mathbf{d}_k, \mathbf{d}_j$ and $\mathbf{D}_k, \mathbf{D}_j$, respectively, we obtain the covariant components $\tilde{k}_{kj} - (\tilde{k}_0)_{kj}$. Because these components are skew-symmetric, there is an associated axial vector with contravariant components

$$k^i(s,t) = \frac{1}{2} e^{ijk} \left(\mathbf{d}_k \cdot \tilde{\mathbf{k}} \mathbf{d}_j - \mathbf{D}_k \cdot \tilde{\mathbf{k}}_0 \mathbf{D}_j \right) = \frac{1}{2} d^{-1/2} \varepsilon_{ijk} (\mathbf{d}_k \cdot \mathbf{d}_{j,s} - \mathbf{D}_k \cdot \mathbf{D}_{j,s}) \tag{38}$$

which is the second strain measure. In the following, we prove that we obtain the internal virtual work expression (30) when varying the elastic potential (36). Using (20) and (A.2), the variation of the first potential takes the form

$$\delta W_1 = \frac{\partial W_1}{\partial \gamma_i} \delta \gamma_i \overset{(37)}{=} \frac{\partial W_1}{\partial \gamma_i} (\delta \boldsymbol{\varphi}_{,s} \cdot \mathbf{d}_i + \boldsymbol{\varphi}_{,s} \cdot \delta \mathbf{d}_i) = \mathbf{n} \cdot (\delta \boldsymbol{\varphi}_{,s} - \delta \boldsymbol{\phi} \times \boldsymbol{\varphi}_{,s}) \, , \tag{39}$$

DOI: 10.1002/nme

where we recognize the resultant contact force $\mathbf{n} = n^i \mathbf{d}_i = \frac{\partial W_1}{\partial \gamma_i} \mathbf{d}_i$. By expansion with the reciprocity condition $\delta^i_j = \mathbf{d}^i \cdot \mathbf{d}_j$ and using (20), the variation of the second potential yields

$$\delta W_2 = \frac{\partial W_2}{\partial k^i} \delta k^i = \frac{\partial W_2}{\partial k^i} \mathbf{d}^i \cdot \delta k^j \mathbf{d}_j = \mathbf{m} \cdot (\delta \mathbf{k} - \delta \boldsymbol{\phi} \times \mathbf{k}) \,. \tag{40}$$

Here, we identify the contact torque as $\mathbf{m} = m_i \mathbf{d}^i = \frac{\partial W_2}{\partial k^i} \mathbf{d}^i$. Comparing (39) and (40) with (30) proves the choice of the strain measures and their corresponding elastic potentials.

Remark 3
The contact force $\mathbf{n}$ and the contact torque $\mathbf{m}$ are naturally represented by covariant directors $\mathbf{d}_i$ and by contravariant directors $\mathbf{d}^i$, respectively. According to the property of the cross product, (3), and the definition of the generalized contact forces (31), these representations are completely reasonable.

We assume the following quadratic form as the elastic potential

$$W\left(\gamma_i, k^i\right) = \frac{1}{2} d^{1/2} \gamma_i \, (\hat{\mathbf{D}}_1)^{ij} \, \gamma_j + \frac{1}{2} d^{1/2} k^i \, (\hat{\mathbf{D}}_2)_{ij} \, k^j \,, \tag{41}$$

with

$$[\hat{\mathbf{D}}_1] = \mathrm{Diag}[GA_1, GA_2, EA] \quad \text{and} \quad [\hat{\mathbf{D}}_2] = \mathrm{Diag}[EI_1, EI_2, GJ] \,, \tag{42}$$

where $[\hat{\mathbf{D}}_1]$ and $[\hat{\mathbf{D}}_2]$ contain the collection of the stiffness components $(\hat{\mathbf{D}}_1)^{ij}$ and $(\hat{\mathbf{D}}_2)_{ij}$, respectively. Consequently, the contact force and the contact torque are

$$\mathbf{n} = n^i \mathbf{d}_i = d^{1/2} (\hat{\mathbf{D}}_1)^{ij} \gamma_j \mathbf{d}_i \,, \quad \mathbf{m} = m_i \mathbf{d}^i = d^{1/2} (\hat{\mathbf{D}}_2)_{ij} k^j \mathbf{d}^i \,. \tag{43}$$

The elastic potential (41) differs from the elastic potential mentioned in Simo & Vu-Quoc [20] by the factor $d^{1/2}$, which is 1, in the case of an orthonormal frame $\{\mathbf{d}_i\}$. As it is shown in Auricchio *et al*. [21], the small-strain constitutive law (43) is motivated by inserting a three-dimensional linear constitutive law into (31), omitting the quadratic terms of the strain, and integrating over the cross section $\bar{A}$. Because $d^{1/2}$ is constant over the cross section $\bar{A}$, the following law for the contact force is obtained

$$\begin{aligned} \mathbf{n} &= \int_{\bar{A}} \mathbf{t}^3 \mathrm{d}^2\theta = \int_{\bar{A}} \boldsymbol{\sigma} \, (\mathbf{g}_1 \times \mathbf{g}_2) \, \mathrm{d}^2\theta \overset{(24)}{=} \int_{\bar{A}} \boldsymbol{\sigma} \, (\mathbf{d}_1 \times \mathbf{d}_2) \, \mathrm{d}^2\theta \overset{(3)}{=} \int_{\bar{A}} \boldsymbol{\sigma} \mathbf{d}^3 d^{1/2} \mathrm{d}^2\theta \\ &= d^{1/2} \int_{\bar{A}} \boldsymbol{\sigma} \mathbf{d}^3 \mathrm{d}^2\theta = d^{1/2} (\hat{\mathbf{D}}_1)^{ij} \gamma_j \, \mathbf{d}_i \,. \end{aligned} \tag{44}$$

The derivation of the contact torque law works analogously.

3.4. Director description

In the subsequent subsection, we describe the rotational degrees of freedom using constraint directors. This formulation leads to a reparametrization of (32). Hence, we reformulate all virtual work contributions that include rotational degrees of freedom such as virtual rotations or curvatures. The internal virtual work due to the contact force is

$$\begin{aligned} \delta W_1^{\mathrm{int}} &= \int_{s_1}^{s_2} \mathbf{n} \cdot [\delta \boldsymbol{\varphi}_{,s} - \delta \boldsymbol{\phi} \times \boldsymbol{\varphi}_{,s}] \mathrm{d}s \overset{(20)}{=} \int_{s_1}^{s_2} \mathbf{n} \cdot \left[\delta \boldsymbol{\varphi}_{,s} + \boldsymbol{\varphi}_{,s} \times \left(\frac{1}{2} \mathbf{d}^i \times \delta \mathbf{d}_i \right) \right] \mathrm{d}s \\ &\overset{(A.3)}{=} \int_{s_1}^{s_2} \left\{ \mathbf{n} \cdot \delta \boldsymbol{\varphi}_{,s} + \frac{1}{2} \left[\left(\mathbf{n} \cdot \mathbf{d}^i \right) \left(\boldsymbol{\varphi}_{,s} \cdot \delta \mathbf{d}_i \right) - \left(\delta \mathbf{d}_i \cdot \mathbf{n} \right) \left(\mathbf{d}^i \cdot \boldsymbol{\varphi}_{,s} \right) \right] \right\} \mathrm{d}s \,. \end{aligned} \tag{45}$$

DOI: 10.1002/nme

With regard to the variation of (17), the internal virtual work of the contact torque takes the form

$$\begin{aligned}\delta W_2^{\text{int}} &= \int_{s_1}^{s_2} \mathbf{m}\cdot[\delta\mathbf{k}-\delta\boldsymbol{\phi}\times\mathbf{k}]\,\mathrm{d}s = \int_{s_1}^{s_2}\mathbf{m}\cdot\delta k^i\mathbf{d}_i\,\mathrm{d}s \\ &= \int_{s_1}^{s_2}\left\{\frac{1}{2}(\mathbf{m}\cdot\mathbf{d}_i)\varepsilon_{ijk}\left[\delta(d^{-1/2})(\mathbf{d}_k\cdot\mathbf{d}_{j,s}) + d^{-1/2}\delta\mathbf{d}_k\cdot\mathbf{d}_{j,s} + d^{-1/2}(\mathbf{d}_k\cdot\delta\mathbf{d}_{j,s})\right]\right\}\mathrm{d}s\,.\end{aligned} \tag{46}$$

The virtual work contribution of the external torques is

$$\delta W_{\overline{\mathbf{m}}}^{\text{ext}} = \int_{s_1}^{s_2}\left\{\delta\mathbf{d}_i\cdot\left(\frac{1}{2}\mathbf{d}^i\times\overline{\mathbf{m}}\right)\right\}\mathrm{d}s + \delta\mathbf{d}_i\cdot\left(\frac{1}{2}\mathbf{d}^i\times\overline{\mathbf{m}}\right)\Big|_{s_1}^{s_2}\,. \tag{47}$$

For the reparametrization of the virtual work contribution of the dynamical forces, it is easier to start directly from the contribution in (6) than from (A.18). Hence,

$$\begin{aligned}\delta W^{\text{dyn}} &= \int_{\overline{\mathrm{B}}}\delta\mathbf{x}\cdot\ddot{\mathbf{x}}\mathrm{d}m = \int_{s_1}^{s_2}\left\{\int_{\bar{\mathrm{A}}}\left[(\delta\boldsymbol{\varphi}+\theta^\alpha\delta\mathbf{d}_\alpha)\cdot\left(\ddot{\boldsymbol{\varphi}}+\theta^\beta\ddot{\mathbf{d}}_\beta\right)\right]\mathrm{d}m\right\}\mathrm{d}s \\ &= \int_{s_1}^{s_2}\left\{\delta\boldsymbol{\varphi}\cdot A_\rho\ddot{\boldsymbol{\varphi}} + \delta\mathbf{d}_\alpha\cdot q_\rho^\alpha\ddot{\boldsymbol{\varphi}} + \delta\boldsymbol{\varphi}\cdot q_\rho^\beta\ddot{\mathbf{d}}_\beta + \delta\mathbf{d}_\alpha\cdot M_\rho^{\alpha\beta}\ddot{\mathbf{d}}_\beta\right\}\mathrm{d}s\,,\end{aligned} \tag{48}$$

with the abbreviation of the time constant inertia coefficients

$$A_\rho(s) = \int_{\bar{\mathrm{A}}}\mathrm{d}m\,,\quad q_\rho^\alpha(s) = \int_{\bar{\mathrm{A}}}\theta^\alpha\mathrm{d}m\,,\quad M_\rho^{\alpha\beta}(s) = \int_{\bar{\mathrm{A}}}\theta^\alpha\theta^\beta\mathrm{d}m\,. \tag{49}$$

As mentioned before, the director description coincides with the geometrically exact beam theory if the director frame remains an orthonormal frame, that is, the following perfect bilateral constraints have to be satisfied at any instant of time

$$g_{ij}(s,t) = \frac{1}{2}(\mathbf{d}_i\cdot\mathbf{d}_j-\delta_{ij}) = 0\,. \tag{50}$$

By the principle of d'Alembert-Lagrange, this will lead to an additional Lagrange multiplier $\lambda^{ij}(s,t)$ in the virtual work expression. The virtual work principle of the geometrically exact beam reparametrized for the variation of directors takes the following form.

$$\begin{aligned}\delta W = \int_{s_1}^{s_2}&\left\{\delta\boldsymbol{\varphi}\cdot\left[A_\rho\ddot{\boldsymbol{\varphi}}+q_\rho^\beta\ddot{\mathbf{d}}_\beta-\overline{\mathbf{n}}\right]+\delta\mathbf{d}_\alpha\cdot\left[M_\rho^{\alpha\beta}\ddot{\mathbf{d}}_\beta+q_\rho^\alpha\ddot{\boldsymbol{\varphi}}\right]-\delta\mathbf{d}_i\cdot\frac{1}{2}\left(\mathbf{d}^i\times\overline{\mathbf{m}}\right)\right. \\ &+\lambda^{ij}\delta\mathbf{d}_i\cdot\mathbf{d}_j+\mathbf{n}\cdot\delta\boldsymbol{\varphi}_{,s}+\frac{1}{2}\left[\left(\mathbf{n}\cdot\mathbf{d}^i\right)\left(\boldsymbol{\varphi}_{,s}\cdot\delta\mathbf{d}_i\right)-\left(\delta\mathbf{d}_i\cdot\mathbf{n}\right)\left(\mathbf{d}^i\cdot\boldsymbol{\varphi}_{,s}\right)\right] \\ &\left.+\frac{1}{2}(\mathbf{m}\cdot\mathbf{d}_i)\varepsilon_{ijk}\left[\delta(d^{-1/2})(\mathbf{d}_k\cdot\mathbf{d}_{j,s})+d^{-1/2}\delta\mathbf{d}_k\cdot\mathbf{d}_{j,s}+d^{-1/2}(\mathbf{d}_k\cdot\delta\mathbf{d}_{j,s})\right]\right\}\mathrm{d}s \\ &-\left(\delta\boldsymbol{\varphi}\cdot\overline{\mathbf{n}}+\delta\mathbf{d}_i\cdot\frac{1}{2}(\mathbf{d}^i\times\overline{\mathbf{m}})\right)\Big|_{s_1}^{s_2}=0\quad\forall\delta\boldsymbol{\varphi},\delta\mathbf{d}_i,t\,.\end{aligned} \tag{51}$$

When we do not distinguish anymore between covariant and contravariant directors, we arrive at the virtual work expression as proposed in [8].

DOI: 10.1002/nme

4. FINITE ELEMENT FORMULATION

To achieve a numerical solution for the constrained problem under consideration, we subdivide the center line $\bar{S} = [s_1, s_2]$ of the beam into a set of finite elements $e \in \mathbb{E} = \{1, \ldots, n_{el}\}$ via

$$\bar{S} = \bigcup_{e \in \mathbb{E}} \bar{S}_e \tag{52}$$

characterized by associated nodal points $A = 1, \ldots, n$, where the position vector of node A is denoted by $\boldsymbol{\varphi}_A$. Then we introduce a polynomial, finite dimensional approximation of the solution space, that is, of the configuration as well as of the director field, as follows

$$\boldsymbol{\varphi}^{\mathrm{h}}(s,t) = \sum_A N^A(s)\boldsymbol{\varphi}_A(t), \quad \mathbf{d}_i^{\mathrm{h}}(s,t) = \sum_A N^A(s)\mathbf{d}_{iA}(t)\,. \tag{53}$$

Using a standard Galerkin type approach, the space of admissible test functions is approximated analogously

$$\delta\boldsymbol{\varphi}^{\mathrm{h}}(s) = \sum_A N^A(s)\delta\boldsymbol{\varphi}_A, \quad \delta\mathbf{d}_i^{\mathrm{h}}(s) = \sum_A N^A(s)\delta\mathbf{d}_{iA}\,, \tag{54}$$

where $N^A(s) : \bar{\mathrm{S}} \to \mathbb{R}$ are global, Lagrange-type shape functions.

Taking the definition of the strain measures (37) and (38) into account, we can write

$$\begin{aligned} \gamma_i^{\mathrm{h}} &= N^A N_{,s}^B \mathbf{d}_{iA}\cdot\boldsymbol{\varphi}_B - N^A N_{,s}^B \mathbf{D}_{iA}\cdot\boldsymbol{\varphi}_{0B} \\ k^{i,\mathrm{h}} &= \frac{1}{2}\det\left(\mathbf{R}^{-1,\mathrm{h}}\right)\varepsilon_{ijk}\left(N^A N_{,s}^B \mathbf{d}_{kA}\cdot\mathbf{d}_{jB} - N^A N_{,s}^B \mathbf{D}_{kA}\cdot\mathbf{D}_{jB}\right) \end{aligned} \tag{55}$$

for their discrete counterparts. Here, the discrete rotation matrix is given by $\mathbf{R}^{\mathrm{h}} = \left[\mathbf{d}_1^{\mathrm{h}}, \mathbf{d}_2^{\mathrm{h}}, \mathbf{d}_3^{\mathrm{h}}\right]$. Note that the matrix $\mathbf{R}^{\mathrm{h}}$ in general is not a proper rotation matrix because of the lack of orthonormality of the discrete director frame caused by interpolation (53). Using the reciprocity condition, the values of the contravariant directors $\mathbf{d}^{i,\mathrm{h}}$ can be extracted from the inverse discrete rotation matrix $\mathbf{R}^{-\mathrm{T,h}} = \left[\mathbf{d}^{1,\mathrm{h}}, \mathbf{d}^{2,\mathrm{h}}, \mathbf{d}^{3,\mathrm{h}}\right]$. The internal virtual work of the contact force (45) reads

$$\begin{aligned} \delta W_1^{\mathrm{int,h}} = {} & \delta\boldsymbol{\varphi}_A \cdot \int_{s_1}^{s_2} N_{,s}^A\,\mathbf{n}^{\mathrm{h}}\,\mathrm{d}s + \\ & \sum_{i=1}^{3}\delta\mathbf{d}_{iA}\cdot\int_{s_1}^{s_2}\frac{1}{2}\left[\left(\mathbf{n}^{\mathrm{h}}\cdot\mathbf{d}^{i,\mathrm{h}}\right)N^A N_{,s}^B\boldsymbol{\varphi}_B - \left(\boldsymbol{\varphi}_{,s}^h\cdot\mathbf{d}^{i,\mathrm{h}}\right)N^A\mathbf{n}^{\mathrm{h}}\right]\mathrm{d}s\,. \end{aligned} \tag{56}$$

Because $d^{-1/2,\mathrm{h}} = \det\left(\mathbf{R}^{-1,\mathrm{h}}\right)$ and $\delta(d^{-1/2}) = \delta\left(\left[\mathbf{d}_1^{\mathrm{h}}\cdot\left(\mathbf{d}_2^{\mathrm{h}}\times\mathbf{d}_3^{\mathrm{h}}\right)\right]^{-1}\right) = -d^{-1,\mathrm{h}}\,\delta\left[\mathbf{d}_1^{\mathrm{h}}\cdot\left(\mathbf{d}_2^{\mathrm{h}}\times\mathbf{d}_3^{\mathrm{h}}\right)\right]$, the internal virtual work of the contact torques (46) follows as

$$\begin{aligned} \delta W_2^{\mathrm{int,h}} = {} & \frac{1}{2}\delta\mathbf{d}_{iA}\cdot\int_{s_1}^{s_2}\det\left(\mathbf{R}^{-1,\mathrm{h}}\right)\left(\mathbf{m}^{\mathrm{h}}\cdot\mathbf{d}_k^{\mathrm{h}}\right)\varepsilon_{kji}\left(N^A N_{,s}^B\mathbf{d}_{jB} - N_{,s}^A N^B\mathbf{d}_{jB}\right)\,\mathrm{d}s \\ & - \frac{1}{2}\delta\mathbf{d}_{1A}\cdot\int_{s_1}^{s_2}\left(\det\left(\mathbf{R}^{-1,\mathrm{h}}\right)\right)^2 N^A\left(\mathbf{d}_2^{\mathrm{h}}\times\mathbf{d}_3^{\mathrm{h}}\right)\left(\mathbf{m}^{\mathrm{h}}\cdot\mathbf{d}_l^{\mathrm{h}}\right)\varepsilon_{lmn}\left(\mathbf{d}_n^{\mathrm{h}}\cdot\mathbf{d}_{m,s}^{\mathrm{h}}\right)\,\mathrm{d}s \\ & - \frac{1}{2}\delta\mathbf{d}_{2A}\cdot\int_{s_1}^{s_2}\left(\det\left(\mathbf{R}^{-1,\mathrm{h}}\right)\right)^2 N^A\left(\mathbf{d}_3^{\mathrm{h}}\times\mathbf{d}_1^{\mathrm{h}}\right)\left(\mathbf{m}^{\mathrm{h}}\cdot\mathbf{d}_l^{\mathrm{h}}\right)\varepsilon_{lmn}\left(\mathbf{d}_n^{\mathrm{h}}\cdot\mathbf{d}_{m,s}^{\mathrm{h}}\right)\,\mathrm{d}s \\ & - \frac{1}{2}\delta\mathbf{d}_{3A}\cdot\int_{s_1}^{s_2}\left(\det\left(\mathbf{R}^{-1,\mathrm{h}}\right)\right)^2 N^A\left(\mathbf{d}_1^{\mathrm{h}}\times\mathbf{d}_2^{\mathrm{h}}\right)\left(\mathbf{m}^{\mathrm{h}}\cdot\mathbf{d}_l^{\mathrm{h}}\right)\varepsilon_{lmn}\left(\mathbf{d}_n^{\mathrm{h}}\cdot\mathbf{d}_{m,s}^{\mathrm{h}}\right)\,\mathrm{d}s\,. \end{aligned} \tag{57}$$

DOI: 10.1002/nme

For the numerical implementation, it is convenient to collect the components $\gamma_i^{\mathrm{h}}, k^{i,\mathrm{h}}$ in the matrices $[\boldsymbol{\gamma}^h]$ and $[\mathbf{k}^{\mathrm{h}}]$, respectively. Using the constitutive laws of (43), the local, discrete contact force and torque are given by

$$\begin{aligned} \mathbf{n}^{\mathrm{h}} &= \mathbf{d}_i^{\mathrm{h}} n^i = \mathbf{R}^{\mathrm{h}} \det\left(\mathbf{R}^{\mathrm{h}}\right) [\hat{\mathbf{D}}_1] \left[\boldsymbol{\gamma}^{\mathrm{h}}\right] , \\ \mathbf{m}^{\mathrm{h}} &= \mathbf{d}^{i,\mathrm{h}} m_i = \mathbf{R}^{-\mathrm{T},\mathrm{h}} \det\left(\mathbf{R}^{\mathrm{h}}\right) [\hat{\mathbf{D}}_2] \left[\boldsymbol{k}^{\mathrm{h}}\right] . \end{aligned} \tag{58}$$

The external as well as the dynamical contributions can be formulated analogously. Note that we apply a reduced integration, that is, a one-point Gauss quadrature for the two-node element to avoid locking effects. At last, we consider the approximation of the Lagrange multipliers associated to the constraints of orthonormality (50). In particular, these constraints are enforced at the nodal points $A = 1, \ldots, n$ leading to the algebraic constraint equations $\boldsymbol{\Phi}_A = \mathbf{0}$. The constraints (50) entail six independent constraint functions per node, which are collected in the vector

$$\boldsymbol{\Phi}_A = \begin{bmatrix} \frac{1}{2}(\boldsymbol{d}_{1A} \cdot \boldsymbol{d}_{1A} - \boldsymbol{D}_{1A} \cdot \boldsymbol{D}_{1A}) \\ \frac{1}{2}(\boldsymbol{d}_{2A} \cdot \boldsymbol{d}_{2A} - \boldsymbol{D}_{2A} \cdot \boldsymbol{D}_{2A}) \\ \frac{1}{2}(\boldsymbol{d}_{3A} \cdot \boldsymbol{d}_{3A} - \boldsymbol{D}_{3A} \cdot \boldsymbol{D}_{3A}) \\ \frac{1}{2}(\boldsymbol{d}_{1A} \cdot \boldsymbol{d}_{2A} - \boldsymbol{D}_{1A} \cdot \boldsymbol{D}_{2A}) \\ \frac{1}{2}(\boldsymbol{d}_{1A} \cdot \boldsymbol{d}_{3A} - \boldsymbol{D}_{1A} \cdot \boldsymbol{D}_{3A}) \\ \frac{1}{2}(\boldsymbol{d}_{2A} \cdot \boldsymbol{d}_{3A} - \boldsymbol{D}_{2A} \cdot \boldsymbol{D}_{3A}) \end{bmatrix} \tag{59}$$

Correspondingly, the Lagrange multipliers are approximated by using Dirac deltas as basis functions $M_A(s)$. Accordingly,

$$\lambda_{ij}^{\mathrm{h}}(s,t) = \sum_A M_A(s) \lambda_{ij}^A(t) \tag{60}$$

This procedure is in accordance with the developments in [8].

Remark 4
Instead of using the method of Lagrange multipliers for the enforcement of the nodal constraints of orthonormality, three nodal rotation parameters could be introduced. This procedure yields a significant size-reduction of the algebraic system of nonlinear equations to be solved. We refer to [8], Section 3.2, for further details. Note, however, that this approach merely reduces the number of unknowns and does not alter the numerical approximation properties of the finite element formulation at hand.

Remark 5
The discrete strain measures emanating from the present approach are frame-indifferent (or objective). This can be verified in a straightforward manner in complete analogy to Section 3 in [8].

5. NUMERICAL INVESTIGATIONS

In this section, we evaluate the accuracy and performance of the newly proposed method. All examples are carried out in a three-dimensional setting, although some of them remain planar. Because the new contribution of the proposed formulation relies on the formulation of the internal virtual work, we demonstrate the performance using static benchmark tests and compare the results with the original director-based formulation in [8]. Throughout all the examples, two-node elements are used.

DOI: 10.1002/nme

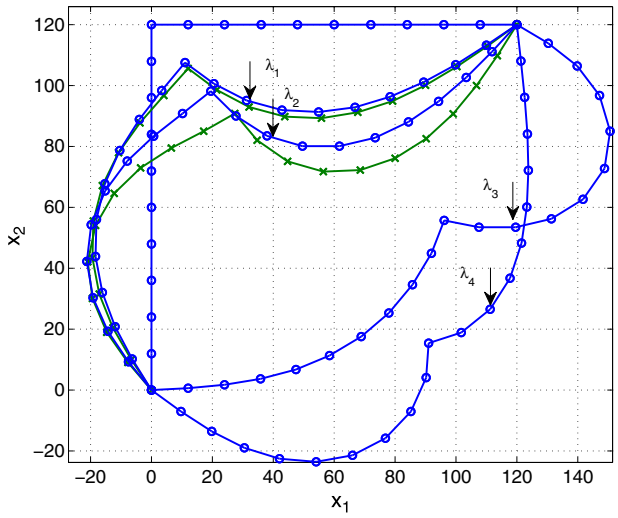

Figure 3. Buckling test, the results of the new approach are marked with o, the results of the original approach with x.

5.1. *Planar equilibrium problem*

In this example, we consider the buckling of a hinged right angle frame. The geometry of the reference configuration is given in Figure 3, the material data for the used model are given as follows: $GA = 16.62 \times 10^6$, $EA = 43.20 \times 10^6$, $EI = 14.40 \times 10^6$, and $GJ = 11.08 \times 10^6$, see also [20]. Dirichlet boundary conditions are applied to the translational degrees of freedom at both ends, such that rotation is possible. Four different loads λ_{1-4} are applied to the frame as dead loads, using $\lambda_1 = -15 \times 10^3 \boldsymbol{e}_2$, $\lambda_2 = -17.4 \times 10^3 \boldsymbol{e}_2$, $\lambda_3 = 9.233 \times 10^3 \boldsymbol{e}_2$, and $\lambda_4 = -21.014 \times 10^3 \boldsymbol{e}_2$. The results of the original director formulation are added for comparison for λ_1 and λ_2. In both loading situations, the new formulation reacts stiffer as the original one; this behavior is closer to the solution as will be shown in a subsequent convergence test, see Section 5.3. Using a standard Newton-Raphson iteration scheme, the snap-through of the buckling problem for the loading λ_3 and λ_4 could only be achieved for the new approach, since the original formulation diverges. An arc-length method would be necessary for the calculation of the results of the original approach. Thus, the new approach is more robust than the original director formulation.

5.2. *Spatial cantilever problem*

The next example consists of a cantilever bending test, see Figure 4. The cantilever is curved in its stress-free reference configuration. In particular, $1/8$ of a circle with radius $R = 100$ in z-direction is used as center line. Different constant loads are applied to the tip at the end of the beam, whereas the other end of the beam at [0, 0, 0] is completely clamped in all directions. The material data are as follows: $GA_1 = GA_2 = 5 \times 10^6$, $EA = 10^7$ and $EI_1 = EI_2 = GJ = 10^7/12$. Table I shows the corresponding results for different numbers of elements. In addition to that, the numerical results corroborate the frame-indifference of the present method (cf. [8]).
As can be seen, the new formulation outperforms the original one for coarse meshes. Furthermore, both approaches converge to the same results.

5.3. *Bending test*

This example consists of a straight beam, clamped at one end, and a moment applied to it at the other end. The length of the beam is $L = 1$ and the material data are as follows: $EA = \frac{1}{25^2}$, $GA = \frac{1}{2.7}\frac{1}{25^2}$, $EI = \frac{1}{12}\frac{1}{25^4}$ and $GJ = \frac{1}{2.7}\frac{1}{6}\frac{1}{25^2}$. An analytical solution for a closed curve exists with $M_o = 2\pi EI/L$, see the snapshots in Figure 5.

DOI: 10.1002/nme

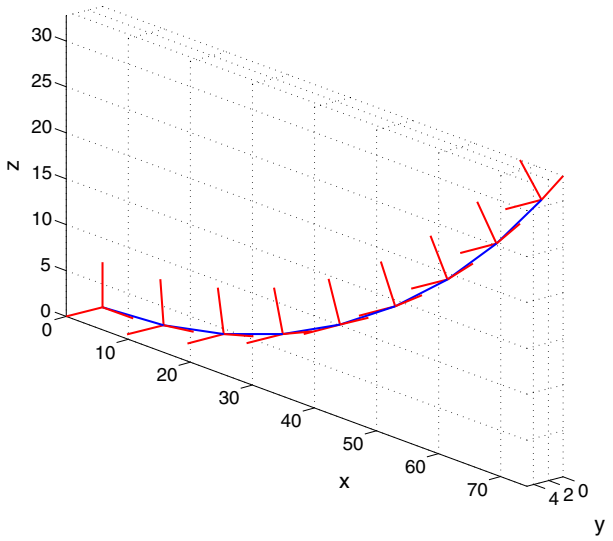

Figure 4. Cantilever problem, reference configuration of the center line and the director triads.

Table I. Tip displacement in $\boldsymbol{e}_2-$ direction.

Load level	Original approach			New approach		
$[F_1,\ F_2,\ F_3]$	8 El.	16 El.	32 El.	8 El.	16 El.	32 El.
[−600, 0, 0]	0	0	0	0	0	0
[−600, 600, 0]	61.3302	60.1177	59.9022	60.1246	59.9033	59.8510
[−600, 600, 600]	40.0323	38.9342	38.7539	38.7966	38.7195	38.7027
[0, 600, 600]	38.3769	37.7264	37.5829	37.5228	37.5316	37.5351
[0, 0, 600]	0	0	0	0	0	0

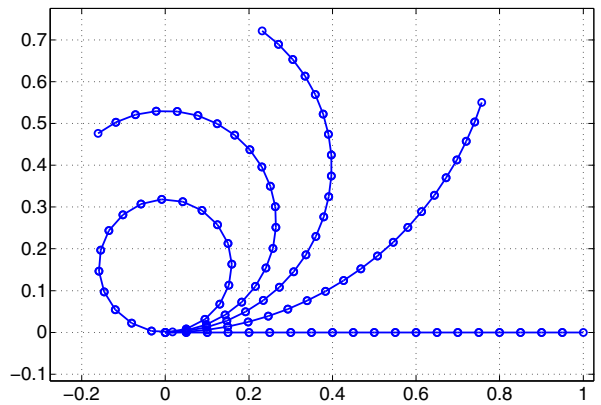

Figure 5. Bending problem, configuration for $M = 0$, $M = \frac{2}{5}M_0$, $M = \frac{4}{5}M_0$, $M = \frac{6}{5}M_0$, and $M = M_0$.

A convergence plot is shown in Figure 6, where the size of the elements is plotted versus the norm of the distance $\|\boldsymbol{d}\|$ between the numerical and the analytical solution of the tip displacement of the beam.

This convergence test shows once again that the new approach clearly outperforms the original formulation. We were able to run this example with a minimum number of two elements, whereas the iterative solution procedure (i.e. Newton's method) does not converge for the original formulation if less than 15 elements are employed.

DOI: 10.1002/nme

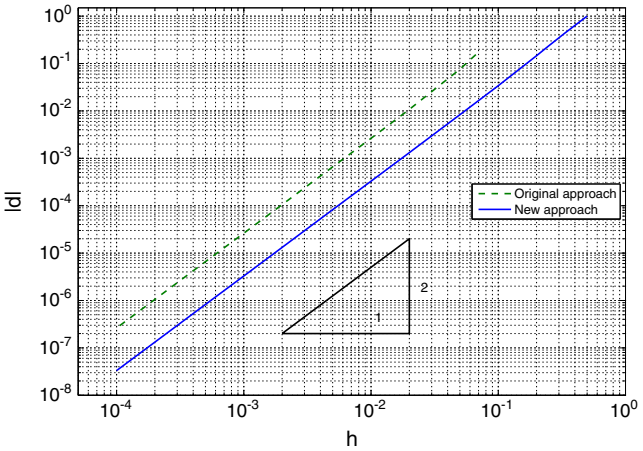

Figure 6. Convergence results for the bending problem.

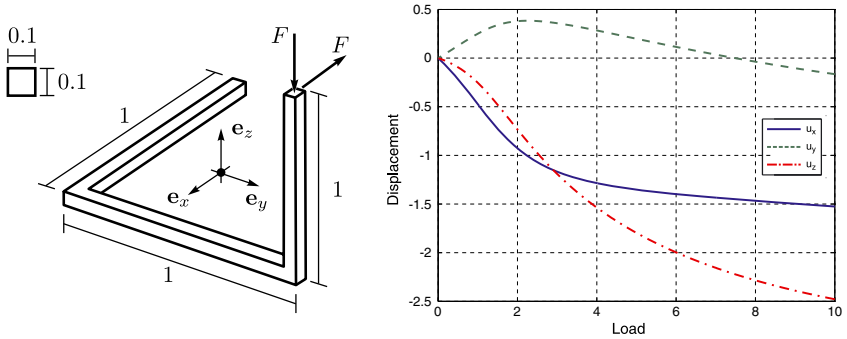

Figure 7. Geometry of the structure and tip displacement versus applied load F.

5.4. Beam with slope discontinuity

This last example demonstrates the capabilities of the proposed approach for non-smooth, three-dimensional geometries, compare with Romero [22]. The structure consists of three, in their reference configuration straight beams of unit length, connected at right angels, see Figure 7. To model the connection of two beams at right angles, we apply six algebraic constraints in complete analogy to the description of shell intersections in [23, Section 6.1]. The material data are as follows: $E = 1 \times 10^6$ and $G = 5 \times 10^5$. Moreover, the beam has a quadratic cross section area of $A = 1 \times 10^{-2}$.

The structure is fully clamped at one end, and two forces with magnitude $F = 10$ are applied in negative $\mathbf{e}_x$- and $\mathbf{e}_z$-direction to the other end. In Figure 7, the displacement of the tip is plotted versus the load F using a total of 12 elements of uniform length and distribution.

Analogous to the bending test, a convergence plot is given in Figure 8 to compare the results of the new approach with the original formulation. We established an error indicator using the distance $\|\boldsymbol{d}\|$ between the numerical solution of the tip displacement for different element numbers and a reference solution with 1920 elements. Note that the norm of the difference in the tip displacement between both approaches for the reference solution is below 2.5×10^{-6}.

Again, the new approach clearly outperforms the original formulation even for the complex three-dimensional problem at hand. The original approach diverges using a total of six elements for the chosen load increment size of $\Delta F = 0.05$, whereas the new approach converges without problems.

DOI: 10.1002/nme

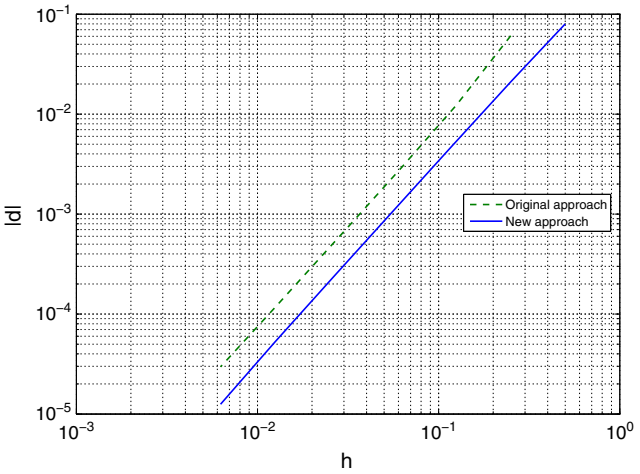

Figure 8. Errors in tip displacements versus h-refinement.

6. CONCLUSIONS

The present approach can be viewed as generalization of the method proposed in [24]. In this work, the director-based formulation of rigid body dynamics is treated. There, the discretization in time generally destroys the orthonormality of the director frame, which is inherently connected to the kinematic assumption of rigidity. It is shown in [24] that the lack of orthonormality of the director frame distorts the application of external torques and thus destroys the balance of angular momentum. This deficiency of the discrete rigid body formulation can be resolved by properly distinguishing between covariant and contravariant directors in much the same way as in the present work.

In particular, the newly proposed formulation of the beam curvature accounts in a natural way for the lack of orthonormality of the director frame caused by the nodal interpolation of the directors. The lack of orthonormality of the director frame can be regarded as a discretization error, which diminishes if the number of elements is increased.

Consequently, the present approach has an especially pronounced effect when course discretizations and low-order finite elements are used. The numerical results presented in Section 5 show indeed a significant improvement over the original implementation of the director-based beam finite element formulation. It has further been verified, both theoretically and numerically, that the present approach yields a consistent discretization of the geometrically exact (Simo-Reissner) beam model. It is also worth noting that in analogy to the original director-based implementation, the present method retains the property of frame-indifference (or objectivity) in the discrete setting.

APPENDIX

Properties of the cross product

The cross product $\times$ as a skew-symmetric operator on $\mathbb{R}^3$ has some useful identities that are used frequently in this paper. In $\mathbb{R}^3$, the cross product fulfills the Jacobi identity

$$\mathbf{a} \times (\mathbf{b} \times \mathbf{c}) + \mathbf{b} \times (\mathbf{c} \times \mathbf{a}) + \mathbf{c} \times (\mathbf{a} \times \mathbf{b}) = 0 \quad \forall \mathbf{a}, \mathbf{b}, \mathbf{c} \in \mathbb{R}^3 . \tag{A.1}$$

The triple product is invariant under even permutation, that is,

$$\mathbf{a} \cdot (\mathbf{b} \times \mathbf{c}) = \mathbf{b} \cdot (\mathbf{c} \times \mathbf{a}) = \mathbf{c} \cdot (\mathbf{a} \times \mathbf{b}) \quad \forall \mathbf{a}, \mathbf{b}, \mathbf{c} \in \mathbb{R}^3 . \tag{A.2}$$

The vector triple product fulfills Grassmann's identity

$$\mathbf{a} \times (\mathbf{b} \times \mathbf{c}) = (\mathbf{a} \cdot \mathbf{c})\mathbf{b} - (\mathbf{a} \cdot \mathbf{b})\mathbf{c} \quad \forall \mathbf{a}, \mathbf{b}, \mathbf{c} \in \mathbb{R}^3 . \tag{A.3}$$

DOI: 10.1002/nme

The quadruple product

$$(\mathbf{a}\times\mathbf{b})\cdot(\mathbf{c}\times\mathbf{d}) = (\mathbf{a}\cdot\mathbf{c})(\mathbf{b}\cdot\mathbf{d}) - (\mathbf{a}\cdot\mathbf{d})(\mathbf{b}\cdot\mathbf{c}) \quad \forall \mathbf{a},\mathbf{b},\mathbf{c},\mathbf{d}\in\mathbb{R}^3\,, \tag{A.4}$$

and another useful identity, where we use the tilde to denote the skew-symmetric tensor to the associated axial vector, is

$$\mathbf{a}\times(\mathbf{b}\times(\mathbf{b}\times\mathbf{a})) = -\mathbf{b}\times(\mathbf{a}\times(\mathbf{a}\times\mathbf{b})) = -\tilde{\mathbf{b}}\tilde{\mathbf{a}}\tilde{\mathbf{a}}\mathbf{b} \quad \forall \mathbf{a},\mathbf{b}\in\mathbb{R}^3\,. \tag{A.5}$$

Skew-symmetry of $\tilde{\mathbf{k}}$

For $d_{ij} = \mathbf{d}_i\cdot\mathbf{d}_j = \text{constant}$, we can show that $\tilde{\mathbf{k}} = \mathbf{R}_{,s}\,\mathbf{R}^{-1} = \mathbf{d}_{k,s}\otimes\mathbf{d}^k$ in the basis of $\mathbf{d}^i\otimes\mathbf{d}^j$ is skew-symmetric. Because $\mathbf{R}\mathbf{R}^{-1} = \mathbf{I}$, it follows directly that

$$\mathbf{d}_{k,s}\otimes\mathbf{d}^k = \mathbf{R}_{,s}\,\mathbf{R}^{-1} = -\mathbf{R}\left(\mathbf{R}^{-1}\right)_{,s} = -\mathbf{d}_k\otimes\mathbf{d}^k{}_{,s}\,. \tag{A.6}$$

By applying $\mathbf{d}_i\cdot(\bullet)\mathbf{d}_j$ to (A.6) and the fact that the symmetric metric $d_{ij} = \text{constant}$, this leads to

$$\mathbf{d}_i\cdot\mathbf{d}_{j,s} = -d_{ik}(\mathbf{d}^k{}_{,s}\cdot\mathbf{d}_j) = -(d_{ik}\mathbf{d}^k)_{,s}\cdot\mathbf{d}_j = -\mathbf{d}_{i,s}\cdot\mathbf{d}_j\,. \tag{A.7}$$

Using (A.7),

$$(-\tilde{\mathbf{k}}^{\mathrm{T}})_{ij} = -\mathbf{d}_i\cdot(\mathbf{d}^k\otimes\mathbf{d}_{k,s})\mathbf{d}_j = -\mathbf{d}_{i,s}\cdot\mathbf{d}_j \overset{(A.7)}{=} \mathbf{d}_i\cdot\mathbf{d}_{j,s} = (\tilde{\mathbf{k}})_{ij}\,, \tag{A.8}$$

which shows the skew-symmetry of $\tilde{\mathbf{k}}$ in the basis of $\mathbf{d}^i\otimes\mathbf{d}^j$. For the basis $\mathbf{d}_i\otimes\mathbf{d}_j$, the proof works analogously.

Proof of identity (26)

Variation and derivative with respect to s commute $(\delta\mathbf{d}_k)_{,s} = \delta(\mathbf{d}_{k,s})$. By (16) and (20), this can be written as

$$(\delta\boldsymbol{\phi}\times\mathbf{d}_k)_{,s} = \delta(\mathbf{k}\times\mathbf{d}_k)\,. \tag{A.9}$$

Applying the product rule and using again (16) and (20) yields

$$(\delta\boldsymbol{\phi})_{,s}\times\mathbf{d}_k + \delta\boldsymbol{\phi}\times(\mathbf{k}\times\mathbf{d}_k) = \delta\mathbf{k}\times\mathbf{d}_k + \mathbf{k}\times(\delta\boldsymbol{\phi}\times\mathbf{d}_k)\,. \tag{A.10}$$

By subtracting the left-hand side from the right-hand side, using the skew-symmetric property of the cross product and the Jacobi identity (A.1), we obtain

$$\begin{aligned}\mathbf{0} &= \delta\mathbf{k}\times\mathbf{d}_k + \mathbf{k}\times(\delta\boldsymbol{\phi}\times\mathbf{d}_k) + \delta\boldsymbol{\phi}\times(\mathbf{d}_k\times\mathbf{k}) - (\delta\boldsymbol{\phi})_{,s}\times\mathbf{d}_k\\ &\overset{(A.1)}{=} \delta\mathbf{k}\times\mathbf{d}_k - \mathbf{d}_k\times(\mathbf{k}\times\delta\boldsymbol{\phi}) - (\delta\boldsymbol{\phi})_{,s}\times\mathbf{d}_k\\ &= (\delta\mathbf{k} - \delta\boldsymbol{\phi}\times\mathbf{k} - (\delta\boldsymbol{\phi})_{,s})\times\mathbf{d}_k\,.\end{aligned} \tag{A.11}$$

Because the right-hand side of (A.11) has to vanish for all directors $\mathbf{d}_k\in\mathbb{E}^3$, we obtain the important identity

$$(\delta\boldsymbol{\phi})_{,s} = \delta\mathbf{k} - \delta\boldsymbol{\phi}\times\mathbf{k}\,. \tag{A.12}$$

Virtual work contributions of external forces

Because the measure $\mathrm{d}\mathbf{f}$ allows for Dirac-type contributions as well, boundary terms do not vanish. Insofar,

$$\delta W^{\mathrm{ext}} = \int_{\overline{\mathrm{B}}}\delta\mathbf{x}\cdot\mathrm{d}\mathbf{f} \overset{(25)}{=} \int_{s_1}^{s_2}(\delta\boldsymbol{\varphi}\cdot\overline{\mathbf{n}} + \delta\boldsymbol{\phi}\cdot\overline{\mathbf{m}})\,\mathrm{d}s + (\delta\boldsymbol{\varphi}\cdot\overline{\mathbf{n}} + \delta\boldsymbol{\phi}\cdot\overline{\mathbf{m}})\,\big|_{s_1}^{s_2}\,, \tag{A.13}$$

DOI: 10.1002/nme

where the generalized external forces $\overline{\mathbf{n}}$ and $\overline{\mathbf{m}}$ are the integrated quantities

$$\overline{\mathbf{n}}(s,t) = \int_{\bar{\mathrm{A}}} \mathrm{d}\mathbf{f}\,, \quad \overline{\mathbf{m}}(s,t) = \int_{\bar{\mathrm{A}}} (\boldsymbol{\rho} \times \mathrm{d}\mathbf{f})\,. \tag{A.14}$$

We want to mention that contact forces on the lateral surfaces contribute on the boundary of $\bar{A}(s)$.

Virtual work contributions of inertia terms

For manipulating the inertia terms, it is convenient to introduce some abbreviations of integral expressions. With $\boldsymbol{\varphi}_c$, in the following, the line of centroids is meant.

$$A_\rho(s) := \int_{\bar{\mathrm{A}}} \mathrm{d}m\,, \quad \mathbf{q} := A_\rho(\boldsymbol{\varphi}_c - \boldsymbol{\varphi}) = \int_{\bar{\mathrm{A}}} \boldsymbol{\rho}\,\mathrm{d}m\,, \quad \mathbf{I}_\rho(s) := \int_{\bar{\mathrm{A}}} \tilde{\boldsymbol{\rho}}\tilde{\boldsymbol{\rho}}^{\mathrm{T}}\mathrm{d}m\,. \tag{A.15}$$

Using the fact that

$$\ddot{\mathbf{q}} = (\boldsymbol{\omega} \times A_\rho(\boldsymbol{\varphi}_c - \boldsymbol{\varphi}))^{\cdot} = \dot{\boldsymbol{\omega}} \times A_\rho(\boldsymbol{\varphi}_c - \boldsymbol{\varphi}) + \boldsymbol{\omega} \times (\boldsymbol{\omega} \times A_\rho(\boldsymbol{\varphi}_c - \boldsymbol{\varphi})) \tag{A.16}$$

and

$$\mathbf{h} = \mathbf{I}_\rho \boldsymbol{\omega}\,, \quad \dot{\mathbf{h}} = \mathbf{I}_\rho \dot{\boldsymbol{\omega}} + \dot{\mathbf{I}}_\rho \boldsymbol{\omega} = \mathbf{I}_\rho \dot{\boldsymbol{\omega}} + \boldsymbol{\omega} \times \mathbf{I}_\rho \boldsymbol{\omega}\,, \tag{A.17}$$

we modify the virtual work expression as follows. The tilde denotes the skew-symmetric tensor to the associated axial vector.

$$\begin{aligned}
\delta W^{\mathrm{dyn}} &= \int_{\overline{\mathrm{B}}} \delta\mathbf{x} \cdot \ddot{\mathbf{x}}\,\mathrm{d}m \overset{(23,25)}{=} \int_{\overline{\mathrm{B}}} \{(\delta\boldsymbol{\varphi} - \tilde{\boldsymbol{\rho}}\delta\boldsymbol{\phi}) \cdot (\ddot{\boldsymbol{\varphi}} - \tilde{\boldsymbol{\rho}}\,\dot{\boldsymbol{\omega}} + \tilde{\boldsymbol{\omega}}\tilde{\boldsymbol{\omega}}\boldsymbol{\rho})\}\,\mathrm{d}m \\
&\overset{(A.15,A.5)}{=} \int_{s_1}^{s_2} \big\{\delta\boldsymbol{\varphi} \cdot \big(A_\rho\ddot{\boldsymbol{\varphi}} + A_\rho[(\boldsymbol{\varphi}_c - \boldsymbol{\varphi})^{\tilde{}}]^{\mathrm{T}}\,\dot{\boldsymbol{\omega}} + \tilde{\boldsymbol{\omega}}\tilde{\boldsymbol{\omega}}A_\rho(\boldsymbol{\varphi}_c - \boldsymbol{\varphi})\big) \\
&\qquad + \delta\boldsymbol{\phi} \cdot \big(A_\rho(\boldsymbol{\varphi}_c - \boldsymbol{\varphi})^{\tilde{}}\ddot{\boldsymbol{\varphi}} + \mathbf{I}_\rho\,\dot{\boldsymbol{\omega}} + \tilde{\boldsymbol{\omega}}\mathbf{I}_\rho\boldsymbol{\omega}\big)\big\}\,\mathrm{d}s \\
&\overset{(A.16,A.17)}{=} \int_{s_1}^{s_2} \Big\{\delta\boldsymbol{\varphi} \cdot \big(A_\rho\ddot{\boldsymbol{\varphi}} + \ddot{\mathbf{q}}\big) + \delta\boldsymbol{\phi} \cdot \Big(\mathbf{q} \times \ddot{\boldsymbol{\varphi}} + \dot{\mathbf{h}}\Big)\Big\}\,\mathrm{d}s\,.
\end{aligned} \tag{A.18}$$

REFERENCES

1. Simo JC. A finite strain beam formulation. The three-dimensional dynamic problem. Part I. *Computer Methods in Applied Mechanics and Engineering* 1985; **49**:55–70.
2. Reissner E. On finite deformations of space-curved beams. *Zeitschrift für Angewandte Mathematik und Physik (ZAMP)* 1981; **32**:734–744.
3. McRobie FA, Lasenby J. Simo–Vu Quoc rods using Clifford algebra. *International Journal for Numerical Methods in Engineering* 1999; **45**:377–398.
4. Bathe KJ, Bolourchi S. Large displacement analysis of three-dimensional beam structures. *International Journal for Numerical Methods in Engineering* 1979; **14**:961–986.
5. Gruttmann F, Sauer R, Wagner W. Theory and numerics of three-dimensional beams with elastoplastic material behaviour. *International Journal for Numerical Methods in Engineering* 2000; **48**:1675–1702.
6. Belytschko T, Liu W, Moran B. *Nonlinear Finite Elements for Continua and Structures*. John Wiley & Sons: Chichester, 2000.
7. Romero I, Armero F. An objective finite element approximation of the kinematics of geometrically exact rods and its use in the formulation of an energy-momentum conserving scheme in dynamics. *International Journal for Numerical Methods in Engineering* 2002; **54**:1683–1716.
8. Betsch P, Steinmann P. Frame-indifferent beam finite elements based upon the geometrically exact beam theory. *International Journal for Numerical Methods in Engineering* 2002; **54**:1775–1788.
9. Betsch P, Steinmann P. Constrained dynamics of geometrically exact beams. *Computational Mechanics* 2003; **31**:49–59.

DOI: 10.1002/nme

10. Romero I. The interpolation of rotations and its application to finite element models of geometrically exact rods. *Computational Mechanics* 2004; **34**:121–133.
11. Betsch P, Steinmann P. A DAE approach to flexible multibody dynamics. *Multibody System Dynamics* 2002; **8**:367–391.
12. Armero F, Romero I. Energy-dissipative momentum-conserving time-stepping algorithms for the dynamics of nonlinear Cosserat rods. *Computational Mechanics* 2003; **31**:3–26.
13. Leyendecker S, Betsch P, Steinmann P. Objective energy-momentum conserving integration for the constrained dynamics of geometrically exact beams. *Computer Methods in Applied Mechanics and Engineering* 2006; **195**:2313–2333.
14. Bauchau OA, Han S. Interpolation of rotation and motion. *Multibody System Dynamics* 2013. (Available from: http://dx.doi.org/10.1007/s11044-013-9365-8).
15. Antman SS. *Nonlinear Problems of Elasticity*, 2nd edition. Springer-Verlag: New York, 2005.
16. Glocker Ch. *Set-Valued Force Laws, Dynamics of Non-Smooth Systems*. Springer-Verlag: Berlin, Heidelberg, 2001.
17. Germain P. The method of virtual power in continuum mechanics. Part 2: Microstructure. *SIAM Journal on Applied Mathematics* 1973; **25**:556–575.
18. Rubin MB. *Cosserat Theories: Shells, Rods and Points*. Kluwer Academic Publishers: Dordrecht, 2000.
19. Schade H, Neemann K. *Tensoranalysis*, Vol. 3. de Gruyter: Berlin, 2009.
20. Simo JC, Vu-Quoc L. A three-dimensional finite-strain rod model. Part II: computational aspects. *Computer Methods in Applied Mechanics and Engineering* 1986; **58**:79–116.
21. Auricchio F, Carotenuto P, Reali A. On the geometrically exact beam model: a consistent, effective and simple derivation from three-dimensional finite-elasticity. *International Journal of Solids and Structures* 2008; **45**:4766–4781.
22. Romero I. A comparison of finite elements for nonlinear beams: the absolute nodal coordinate and geometrically exact formulations. *Multibody System Dynamics* 2008; **20**:51–68.
23. Betsch P, Sänger N. On the use of geometrically exact shells in a conserving framework for flexible multibody dynamics. *Computer Methods in Applied Mechanics and Engineering* 2009; **198**:1609–1630.
24. Betsch P, Sänger N. On the consistent formulation of torques in a rotationless framework for multibody dynamics. *Computers and Structures* 2013; **127**:29–38.

DOI: 10.1002/nme